An Automated MR Image Segmentation System Using Multi-layer Perceptron Neural Network

Amiri S[1], Movahedi MM[1*], Kazemi K[2], Parsaei H[1]

[1]Department of Medical Physics and Biomedical Engineering, School of Medicine, Shiraz University of Medical Sciences, Shiraz, Iran
[2]Department of Electrical and Electronics Engineering, Shiraz University of Technology, Shiraz, Iran

ABSTRACT

Background: Brain tissue segmentation for delineation of 3D anatomical structures from magnetic resonance (MR) images can be used for neuro-degenerative disorders, characterizing morphological differences between subjects based on volumetric analysis of gray matter (GM), white matter (WM) and cerebrospinal fluid (CSF), but only if the obtained segmentation results are correct. Due to image artifacts such as noise, low contrast and intensity non-uniformity, there are some classification errors in the results of image segmentation.

Objective: An automated algorithm based on multi-layer perceptron neural networks (MLPNN) is presented for segmenting MR images. The system is to identify two tissues of WM and GM in human brain 2D structural MR images. A given 2D image is processed to enhance image intensity and to remove extra cerebral tissue. Thereafter, each pixel of the image under study is represented using 13 features (8 statistical and 5 non- statistical features) and is classified using a MLPNN into one of the three classes WM and GM or unknown.

Results: The developed MR image segmentation algorithm was evaluated using 20 real images. Training using only one image, the system showed robust performance when tested using the remaining 19 images. The average Jaccard similarity index and Dice similarity metric for the GM and WM tissues were estimated to be 75.7 %, 86.0% for GM, and 67.8% and 80.7%for WM, respectively.

Conclusion: The obtained performances are encouraging and show that the presented method may assist with segmentation of 2D MR images especially where categorizing WM and GM is of interest.

Keywords

Image segmentation, Artificial neural networks, Multi-layer perceptron

Introduction

Image segmentation is the task of partitioning a digital image into multiple segments such that the pixels assigned to a region, with respect to some characteristic or computed property, are as similar as possible and the objects assigned to different clusters are as different as possible. In medical imaging, the results of image segmentation can assist with locating tumors and other pathologies, measuring tissue volumes, studying anatomical structure and diagnosing several disorders [1]. For example, brain tissue segmentation for delineation of 3D anatomical structures from magnetic resonance (MR) images plays an important role for several applications such as neuro-degenerative disorders [2-3], characterizing morphological differences between subjects based on volumetric analysis of gray matter (GM), white matter (WM)

*Corresponding author:
MM Movahedi
Department of Medical Physics and Biomedical Engineering, School of Medicine, Shiraz University of Medical Sciences, Shiraz, Iran
E-mail: mehdi_movahedi@yahoo.com

and cerebrospinal fluid (CSF) [4-6]. However, these are achieved only if the results of image segmentation are correct. Because of image artifacts such as presence of noise, low contrast and intensity non-uniformity (bias), there are some classification errors in the results of image segmentation. Consequently, image segmentation is still a challenging task in medical image processing [7].

In general, segmentation techniques applied to 2D structural MR images can be categorized as user-dependent method, semi-automatic or automatic. In the user-dependent methods, an expert manually identifies brain tissues in a given MR image using some basic techniques. Histogram thresholding [8-10], region growing [11], region splitting and merging [11], and edge tracing are example of these methods. Such methods are quite subjective, inaccurate, related to the experience and skill of the operator.

Semi-automatic methods are more powerful than the manual methods and utilize many of the same techniques used in automatic methods to reduce the operator's roles and ultimately increase the accuracy of the segmentation algorithm. Clustering-based methods [12-13], Markove model-based methods [14], algorithms developed based on deformable models [15-16] are examples of current semi-automatic image segmentation algorithms. Although these methods are more robust than manual segmentation methods, their performance still depends on their user defined parameters. For example, the performance of the clustering-based algorithms is related to the number of clusters and the initial centers of the clusters set by the operator.

With automatic methods, the process of identifying different regions of the brain in a given MR image is completed automatically. These methods, in general, use the knowledge, information and rules provided by the experts to develop a robust automated algorithm for segmenting a given image. Rule-based methods, supervised classification-based methods, and methods developed based on shape models[17] are examples of automatic image segmentation based algorithms. The common issue of the above systems is that their accuracies are not high enough to be accepted as a reliable clinical decision support system.

Recently, artificial neural networks have been successfully applied for automatic image processing [18].One particular application area where neural networks show promising results is segmentation of 2D cerebral MR images. Multi-layer perceptron have been applied successfully in some difficult problems by training them in supervised manner. In this paper an automated algorithm based on multi-layer perceptron neural network (MLPNN) is presented for segmenting MR images. The proposed system is to identify two tissues of WM and GM in human brain 2D structural MR images.

Methods

The proposed algorithm contains three main stages: pre-processing, feature extraction and classification. The block diagram of the algorithm is shown in figure 1. Detailed description of each step is provided in the following three subsections.

Pre-processing

Segmentation of the MRI images with a high degree of accuracy depends on several factors such as contrast between tissues, resolution between tissues, signal to noise ratio and intensity non- uniformity of tissue. Intensity non-uniformity is the changes in the intensity of the image that are due to non-uniformity in RF coil, non-uniformity in bias magnetic field in imaging system or the position of the sick during imaging that cause the same structure and anatomical tissue in the whole image from an intensity point of view to be different. This non-uniformity in general will reduce the accuracy of segmentation results obtained using either manual methods or automatic methods. Consequently, before segmenting a given im-

age, it must be first pre-processed to reduce the effect of the discussed artifacts. In this paper the FSL software was used for correcting intensity non-uniformity. Figure 2 shows the correction of non-uniformity using the FSL software [19].

Non-brain tissue such as bones; muscles membrane and fat that may exist in a given MRI image can also reduce the accuracy of segmentation. Specifically, such tissues reduce the accuracy of the segmentation algorithm in correctly labeling white matter tissue in the image under study. Therefore, these tissues must be removed from the image. In this paper all non-brain tissues and skull are stripped by bet software integrated in FSL [20].

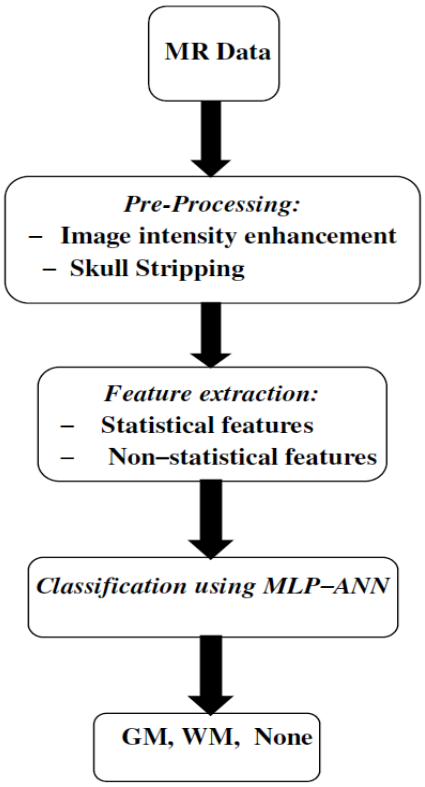

Figure 1: Block diagram of the proposed method

Feature Extraction

Thirteen features were used to represent each pixel of the given image and ultimately for classification purpose. Features are used based on their capability to discriminate between WM and GM tissues. In this work, both statistical and non-statistical features are used for this purpose. For a given pixel (x,y) in the image with gray level $I(x,y)$ eight statistical features and five non-statistical features were estimated from a $(2K+1)\times(2K+1)$ sliding window centered around the pixel. Following are the description of each feature.

Statistical Features

Statistical features in fact represent the statistical parameters of the intensity of a given pixel. Both first order statistical features and second order statistical features are employed here. Intensity, mean, median and standard deviation are the first order statistical features used in this paper. In terms of second statistical features, energy, contrast, entropy and correlation are the features employed [21]. These features in fact compare the difference between the intensity of the target pixel and

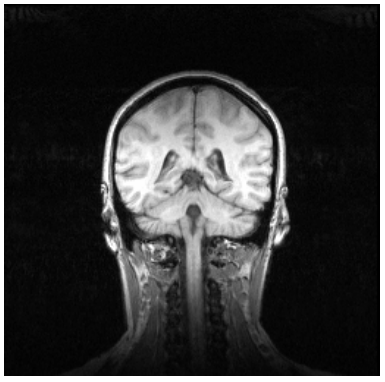

(a)

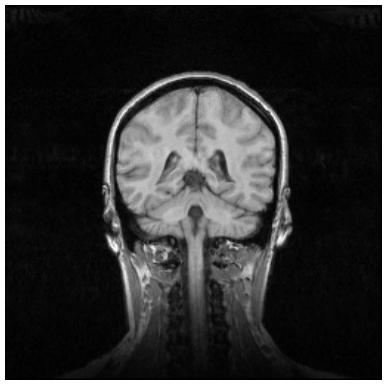

(b)

Figure 2: Correcting intensity non-uniformity. (a) Original image, (b)Correction of non-uniformity using the FSL software.

that of the pixels in a specified region.

Pixel intensity mean, and standard deviation: the mean (μ) and standard deviation(σ) features for each pixel are calculated as:

$$\mu = \frac{1}{(2k+1)^2} \sum_{m=-k}^{k} \sum_{n=-k}^{K} I(x+m, y+n) \quad (1)$$

$$\sigma = \sqrt{\frac{1}{(2k+1)^2} \sum_{m=-k}^{k} \sum_{n=-k}^{K} (I(x+m, y+n) - \mu)^2} \quad (2)$$

where k specifies the size of the window.

Energy is the performance index for image uniformity that is a good quality to manifest the disorder and entropy in the image. If it grows to increase, it means that the intensity will be changed slightly.

$$Energy = \sum_{m=-k}^{k} \sum_{n=-k}^{K} [I(x+m, y+n)]^2 \quad (3)$$

Contrast expresses the rate of local changes in the image. The high value of the contrast expresses the high local changes in the region of the interest.

$$Contrast = \sum_{m=-k}^{k} \sum_{n=-k}^{K} [x+m-(y+n)]^2 I(x+m, y+n) \quad (4)$$

Entropy is a statistical measure of randomness. This parameter is estimated as:

$$Entropy = \sum_{m=-k}^{k} \sum_{n=-k}^{K} I(x+m, y+n) \log(I(x+m, y+n)) \quad (5)$$

Correlation is another parameter used to measure randomness in a given image. This parameter can also be used to estimate the similarity between a given pixel and other pixels of the image. Correlation is zero in random images.

$$Correlation = \sum_{m=-k}^{k} \sum_{n=-k}^{k} (x+m-\mu_x)(y+n-\mu_y) \frac{I(x+m, y+n)}{\sigma_x \sigma_y} \quad (6)$$

where μ_x, μ_y, σ_x and σ_y are estimated using the following four equations.

$$\mu_x = \sum_{m=-k}^{k} \sum_{n=-k}^{k} (x+m) I(x+m, y+n) \quad (7)$$

$$\mu_y = \sum_{m=-k}^{k} \sum_{n=-k}^{k} (y+n) I(x+m, y+n) \quad (8)$$

$$\sigma_x = \sum_{m=-k}^{k} \sum_{n=-k}^{k} \sum_{y} (x+m-\mu_x)^2 I(x+m, y+n) \quad (9)$$

$$\sigma_y = \sum_{m=-k}^{k} \sum_{n=-k}^{k} \sum_{y} (y+n-\mu_y)^2 I(x+m, y+n) \quad (10)$$

Non-Statistical Feature

For non-statistical features, the first and second order geometric moment that are widely used in image processing, pattern identification and artifact recognition were employed. The geometric moment of (p+q) order for a given pixel located at (x,y) in the image is calculated by Equation 11 in which L, M, N are the dimensions of the image[22-23].

$$m_{pq} = \sum_{m=-k}^{k} \sum_{n=-k}^{k} (x+m)^p (y+n)^q I(x+m, y+n) \quad , \quad p,q = 1,2,... \quad (11)$$

Classification

A multi-layer Perceptron Neural Network (MLPNN) were used to estimate the class label of a given pixel and ultimately determine WM and GM tissue in the given image.

A key point in developing a classifier using MLPNN is determining the number of neurons in the hidden layer. High number of this parameter causes over fitting of the trained system and consequently high generalization error. In contrast, low number of neurons in the hidden layer decreases the complexity of the network and prevents over fitting of the network, but the trained network may not provide high accuracy value. In this work, this parameter was estimated using cross validation method. Testing error for different values for the number of neurons in the hidden layer was estimated and the value that provided the minimum testing error was chosen. In this work, the MLPNN with 50 neurons in its hidden layer performed the best. The MLPNN employed was trained by using back propagation algorithm [24].

Quantitative Evaluation

As with any supervised image segmentation algorithm, training and testing a developed

MRI image segmentation algorithm requires reference data (i.e., images whose WM and GM are determined).

For this work, the brain MRI data of 20 normal individuals provided by the morphometric analysis center at a public hospital in Massachusetts are employed. These images along with their segmentation results provided by specialist are available at http://www.nitrc.org/projects/ibsr. This data base known as IBSR data base includes real MRI images that cover different levels of challenges and artifacts of image segmentation such as the low contrast of the image, brain images with small volume of brain and also significant intensity non- uniformity.

Considering the segmentation results provided by the experts as gold standard, the quantitatively assessment of the accuracy of the proposed method was done using two commonly used measures: Dice similarity index (DI) [25] and Jaccard similarity index (JI) [26]. The similarity metrics represent overlap between segmented tissues (A) and corresponding ground truth (G).

$$DI\ \% = \frac{2|A \cap G|}{(|A| + |G|)} \times 100 \qquad (12)$$

$$JI\ \% = \frac{|A \cap G|}{|A \cup G|} \times 100 \qquad (13)$$

Results and Discussion

The developed MLPNN-based image segmentation system were trained using one image of the 20 images discussed in the previous section and were tested on the remaining images. Out of these images an image which has the best signal to noise ratio was used for training the MLPNN and the rest of the images were used for testing. In fact, the network was trained using easy-to-segment image and was tested using difficult-to-segment images. The presented results were obtained with a MLPNN having three layers and 50 neurons in its hidden layer. The network was trained using back propagation algorithm. The parameter K was set to 1, i.e., a square 3×3 window was used in estimating the feature values for a pixel. The values for these two parameters were found experimentally.

The performance of the developed MRI image segmentation system is summarized in table 1. As shown, overall, the developed system performed well in correctly determining GM and WM in the images used. For most of the images used, the DI performance index is greater than 80.0% which shows that at least 80% of the pixels in these images were correctly classified by the developed system.

Figures 3 and 4 show the application of the

Table 1: The performance of the proposed method applied to several images of the IBSR Data base

	DI (%)		JI (%)	
Image	**GM**	**WM**	**GM**	**WM**
100_23	91.7	85.0	84.7	73.9
111_2	84.9	82.3	73.8	70.1
191_3	88.1	83.6	78.7	71.8
202_3	90.3	85.0	82.3	73.9
110_3	83.9	78.9	72.4	65.2
112_2	82.2	78.3	69.7	64.2
17_3	88.5	82.4	79.3	70.0
12_3	85.9	82.2	75.2	69.7
11_3	86.2	82.0	75.7	69.5
15_3	85.4	78.0	74.5	64.0
16_3	80.6	75.7	67.6	60.9
205_3	84.8	82.5	73.6	70.2
13_3	90.5	86.2	82.7	75.7
5_8	84.2	73.1	72.7	57.6
7_8	87.9	82.9	78.5	70.8
6_10	80.6	76.1	67.5	61.4
2_4	86.6	80.7	76.4	67.6
4_8	86.8	78.1	76.7	64.0
8_4	87.1	81.2	77.2	68.2
Mean	**86.1**	**80.7**	**75.7**	**67.8**
STD	**3.1**	**3.5**	**4.7**	**4.9**

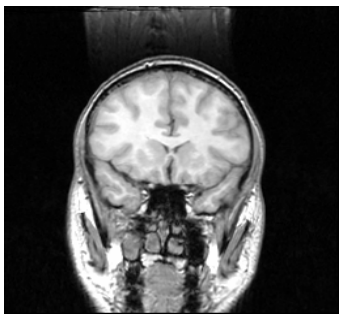

(a) Original image

(b) Manually segmented GM and WM

(c) Segmented GM and WM using proposed method

Figure 3: Segmentation results for MR image ISBR_13_13. (a) original image, (b) manually segmented, and (c) segmented using the proposed method.

proposed method for brain tissue segmentation to a selected slice of the image of subjects 13_3 and 202_3, respectively. As shown, the proposed system performed well in identifying WM and GM and the obtained results are close to that provided by the expert.

Conclusions

Segmenting an MRI image may results in some classification errors and ultimately determining GM and WM in a given image mainly due to image artifacts such as presence of noise, low contrast and intensity non-uniformity. Such errors may mislead the specialists who use the image segmentation results for either clinical or research purpose; Therefore, developing a robust image segmentation algorithm is still a demanding task in medical image processing. In this paper, an automated MRI segmentation algorithm to identify GM and WM in a given MRI image is presented. The system estimates the class label of each pixel in a given MRI image using a MLPNN that is fed by thirteen features (8 statistical and 5 non-statistical) representing pixel. The effectiveness of the developed MR image seg-

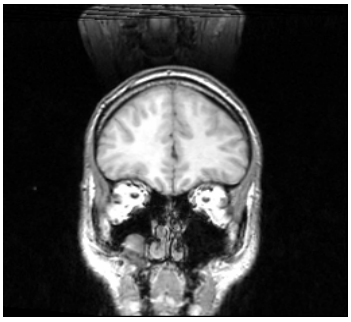

(a) Original image

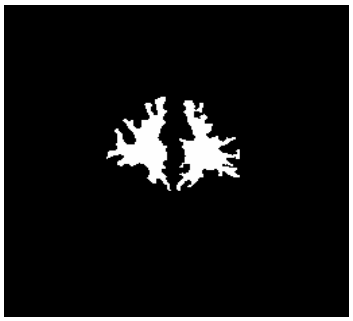

(b) Manually segmented GM and WM

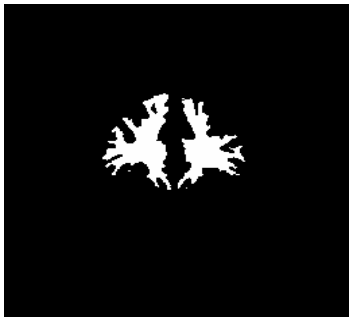

(c) Segmented GM and WM using proposed method

Figure 4: Segmentation results for MR image ISBR_202_3. (a) Original image, (b) manually segmented, and (c) segmented using the proposed method.

mentation algorithm in identifying WM and GM in 2D slice of human brain structural MR images was evaluated using 20 real images. Training using only one image, the system showed robust performance when tested using the remaining 19 images. The average Dice similarity metric and Jaccard similarity index for the GM class was estimated to be 86.0% and 75.7 %, respectively. Likewise, for the WM tissue the achieved average Dice similarity metric and Jaccard similarity index were 80.7% and 67.8% respectively. The obtained performances are encouraging and show that the presented method may assist with segmentation of 2D MR images especially where categorizing WM and GM is of interest.

Conflict of Interest

None

References

1. Pham DL, Xu C, Prince JL. Current Methods in Medical Image Segmentation. *Annu Rev Biomed Eng.* 2000;**2**:315-37. Review. PubMed PMID: 11701515.
2. Tanabe JL, Amend D, Schuff N, DiSclafani V, Ezekiel F, Norman D, et al. Tissue segmentation of the brain in Alzheimer disease. *AJNR American J Neuroradiol.* 1997;**18**:115-23. PubMed PMID: 9010529.

3. Apostolova LG, Dinov ID, Dutton RA, Hayashi KM, Toga AW, Cummings JL, et al. 3D comparison of hippocampal atrophy in amnestic mild cognitive impairment and Alzheimer's disease. *Brain.* 2006;**129**:2867-73. doi: 10.1093/brain/awl274. PubMed PMID: 17018552.
4. Lawrie SM, Abukmeil SS. Brain abnormality in schizophrenia. A systematic and quantitative review of volumetric magnetic resonance imaging studies. *British J Psychiatry.* 1998;**172**:110-20. PubMed PMID: 9519062.
5. McCarley RW, Wible CG, Frumin M, Hirayasu Y, Levitt JJ, Fischer IA, et al. MRI anatomy of schizophrenia. *Biol Psychiatry.* 1999;**45**:1099-119. PubMed PMID: 10331102; PubMed Central PMCID: PMC2846838.
6. Shenton ME, Kikinis R, Jolesz FA, Pollak SD, LeMay M, Wible CG, et al. Abnormalities of the left temporal lobe and thought disorder in schizophrenia. A quantitative magnetic resonance imaging study. *England J Med.* 1992;**327**:604-12. doi: 10.1056/nejm199208273270905. PubMed PMID: 1640954.
7. Cocosco CA, Zijdenbos AP, Evans AC. A fully automatic and robust brain MRI tissue classification method. *Med Image Anal.* 2003;**7**:513-27. PubMed PMID: 14561555.
8. Joliot M, Mazoyer BM. Three-dimensional segmentation and interpolation of magnetic resonance brain images. *IEEE Trans Med Imag.* 1993;**12**:269-77. doi: 10.1109/42.232255. PubMed PMID: 18218414.
9. Suzuki H, Toriwaki J. Automatic segmentation of head MRI images by knowledge guided thresholding. *Computerized medical imaging and graphics.* 1991;**15**:233-40. PubMed PMID: 1913574.
10. Sahoo PK, Soltani S, Wong AKC, Chen YC. A survey of thresholding techniques. *Computer Vision, Graphics, and Image Processing.* 1988;**41**:233-60. doi: 10.1016/0734-189x(88)90022-9.
11. Gonzalez R, Wintz P. *Digital image processing.* 5th ed. New York: Addison-Wesley Publishing Co; 2008.
12. Balafar MA, Ramli AR, Saripan MI, Mahmud R, Mashohor S. Medical image segmentation using Fuzzy C-Mean (FCM) and dominant grey levels of image. In: IEEE *Xplore*, editor. Visual Information Engineering, 2008, 5th International Conference on; 2008 July 29; Xian, China. Hong Kong: IET; 2008. p. 314-7.
13. Bezdek JC, Hall LO, Clarke LP. Review of MR image segmentation techniques using pattern recognition. *Med Phys.* 1993;**20**:1033-48. PubMed PMID: 8413011.
14. Manjunath BS, Chellappa R. Unsupervised texture segmentation using Markov random field models. *IEEE Trans Pattern Anal Mach Intell.* 1991;**13**:478-82. doi: 10.1109/34.134046.
15. Kass M, Witkin A, Terzopoulos D. Snakes: Active contour models. *IInt J Comput Vision.* 1988;**1**:321-31.
16. Wang L, Chen Y, Pan X, Hong X, Xia D. Level set segmentation of brain magnetic resonance images based on local Gaussian distribution fitting energy. *J Neurosci Meth.* 2010;**188**:316-25. doi: 10.1016/j.jneumeth.2010.03.004. PubMed PMID: 20230858.
17. Withey D, Koles Z. A review of medical image segmentation: methods and available software. *Int J Bioelectromagn.* 2008;**10**:125-48.
18. Egmont-Petersen M, de Ridder DD, Handels H. Image processing with neural networks-a review. *Pattern Recognition.* 2002;**35**:2279-301. doi: http://dx.doi.org/10.1016/S0031-3203(01)00178-9.
19. Zhang Y, Brady M, Smith S. Segmentation of Brain MR Images through a Hidden Markov Random Field Model and the Expectation Maximization Algorithm. *IEEE Trans Med Imaging.* 2001;**20**:45-57.
20. Smith SM. Fast robust automated brain extraction. *Human brain mapping.* 2002;**17**:143-55. doi: 10.1002/hbm.10062. PubMed PMID: 12391568.
21. Smith SM, Jenkinson M, Woolrich MW, Beckmann CF, Behrens TE, Johansen-Berg H, et al. Advances in functional and structural MR image analysis and implementation as FSL. *NeuroImage.* 2004;**23**:208-19. doi: 10.1016/j.neuroimage.2004.07.051. PubMed PMID: 15501092.
22. Lo CH, Don HS. 3-D Moment Forms: Their Construction and Application to Object Identification and Positioning. *IEEE Trans Pattern Anal Mach Intell.* 1989;**11**:1053-64.
23. Rizon M, Yazid H, Saad P, *et al.* Object Detection using Geometric Invariant Moment. *Am J Appl Sci.* 2006;**2**:1876-8.
24. Johansson EM, Dowla FU, Goodman DM. Backpropagation learning for multilayer feed-forward neural networks using the conjugate gradient methods. *Int J Neural Sys.* 1991;**2**:1-10.
25. Dice LR. Measures of the Amount of Ecologic Association between Species. *Ecology.* 1945;**26**:297-302.
26. Jaccard P. The Distribution of Flora in the Alpine Zone. *New Phytologist.* 1912;**11**:37-50.